Note: This copy is for your personal non-commercial use only. To order presentation-ready copies for distribution to your colleagues or clients, contact us at www.rsna.org/rsnarights.

RadioGraphics

Uncommon Primary Pelvic Retroperitoneal Masses in Adults: A Pattern-based Imaging Approach[1]

Alampady K. Shanbhogue, MD • Najla Fasih, FRCR • David B. Macdonald, MD • Adnan M. Sheikh, MD • Christine O. Menias, MD Srinivasa R. Prasad, MD

ONLINE-ONLY CME

See www.rsna.org/education/rg_cme.html

LEARNING OBJECTIVES

After completing this journal-based CME activity, participants will be able to:

- List the various uncommon primary pelvic retroperitoneal masses seen in adults.
- Discuss the imaging features of these masses, with emphasis on masses that are unique to the pelvis.
- Describe a pattern-based approach that enables the radiologist to narrow the differential diagnosis.

TEACHING POINTS

See last page

There is a broad spectrum of primary pelvic retroperitoneal masses in adults that demonstrate characteristic epidemiologic and histopathologic features and natural histories. These masses may be classified into five distinct subgroups using a pattern-based approach that takes anatomic distribution and certain imaging characteristics into account, allowing greater accuracy in their detection and characterization and helping to optimize patient management. The five groups are cystic (serous and mucinous epithelial neoplasms, pelvic lymphangioma, tailgut cyst, ancient schwannoma), vascular or hypervascular (solitary fibrous tumor, paraganglioma, pelvic arteriovenous malformation, Klippel-Trénaunay-Weber syndrome, extraintestinal GIST [gastrointestinal stromal tumor]), fat-containing (lipoma, liposarcoma, myelolipoma, presacral teratoma), calcified (calcified lymphocele, calcified rejected transplant kidney, rare sarcomas), and myxoid (schwannoma, plexiform neurofibroma, myxoma). Cross-sectional imaging modalities help differentiate the more common gynecologic neoplasms from more unusual masses. In particular, the tissue-specific multiplanar capability of high-resolution magnetic resonance imaging permits better tumor localization and internal characterization, thereby serving as a road map for surgery.

©RSNA, 2012 • *radiographics.rsna.org*

Abbreviations: AVM = arteriovenous malformation, GIST = gastrointestinal stromal tumor, MIBG = metaiodobenzylguanidine, SFT = solitary fibrous tumor

RadioGraphics 2012; 32:795–817 • **Published online** 10.1148/rg.323115020 • **Content Codes:** CT GI MR

[1]From the Department of Radiology, University of Texas Health Science Center at San Antonio, 7703 Floyd Curl Dr, San Antonio, TX 78229 (A.K.S.); Department of Radiology, Ottawa Hospital, Ottawa, Ont, Canada (N.F., D.B.M., A.M.S.); Mallinckrodt Institute of Radiology, Washington University School of Medicine, St Louis, Mo (C.O.M.); and Department of Radiology, University of Texas M. D. Anderson Cancer Center, Houston, Tex (S.R.P.). Presented as an education exhibit at the 2009 RSNA Annual Meeting. Received February 7, 2011; revision requested July 21 and received November 18; accepted December 7. For this journal-based CME activity, the authors, editor, and reviewers have no relevant relationships to disclose. **Address correspondence to** A.K.S. (e-mail: *shanbhogue@uthscsa.edu*).

©RSNA, 2012

Introduction

The pelvic retroperitoneum forms a part of the pelvic extraperitoneal space but is less well understood than the abdominal retroperitoneum. Experimental studies have provided greater understanding of the anatomy of the three intercommunicating potential extraperitoneal spaces in the pelvis, namely, the prevesical, perivesical, and perirectal spaces (1). The prevesical space is a large potential space that lies between the infraumbilical lower anterior abdominal wall anteriorly and the umbilicovesical fascia posteriorly (2). The perivesical space is located below the pelvic peritoneal reflection, is surrounded by the umbilicovesical fascia, and contains the urinary bladder, uterus (in females), urachus, and obliterated umbilical arteries (2). The perirectal space surrounds the rectum and is divided into the central retrorectal space and the peripheral presacral space by the intervening presacral fascia (3). The pelvic retroperitoneal space referred to in this article includes *(a)* the region within the pelvis posterior to the parietal peritoneal reflection, and *(b)* the presacral and retrorectal spaces (Fig 1). Familiarity with the anatomy of the pelvic extraperitoneal space is essential for identifying the cause of pelvic collections and understanding the spread of disease. In addition, a variety of masses arise primarily within the pelvic retroperitoneum. Anatomically, this potential space contains the iliac vessels, lymphatic vessels, nerves, lymph nodes, and connective tissue. Common disease entities encountered in the pelvic retroperitoneum include lymphadenopathy (metastases or lymphoma); abscess; hematoma; and extension of primary rectal, ureteric, or sacral disease entities. Primary masses of the pelvic retroperitoneum are rare but can arise from any of its anatomic components.

Because ovarian and uterine masses are quite common, a gynecologic cause is typically suspected when a pelvic mass is encountered. Pelvic retroperitoneal masses are often asymptomatic. Their relative rarity and the lack of familiarity with the anatomy and pathologic processes of the pelvic retroperitoneum add to the diagnostic dilemma. There have been several reports of pelvic retroperitoneal masses being mistaken for gynecologic masses at clinical examination and preoperative imaging (4–6). The accurate preoperative differentiation of an extraperitoneal pelvic mass from an intraperitoneal mass (most of which are gynecologic in nature) has significant therapeutic implications, including surgical planning (ie, deciding whether a transperitoneal or a retroperitoneal approach is to be used).

In this article, we describe the classification of selected uncommon primary pelvic retroperitoneal masses seen in adult patients into five distinct subsets on the basis of their predominant or characteristic internal features, an approach that allows greater accuracy in detection and characterization of masses and helps to optimize patient management. These masses are categorized as either cystic (serous and mucinous epithelial neoplasms, pelvic lymphangioma, tailgut cyst, ancient schwannoma), vascular or hypervascular (solitary fibrous tumor [SFT], paraganglioma, pelvic arteriovenous malformation [AVM], Klippel-Trénaunay-Weber syndrome, extraintestinal GIST [gastrointestinal stromal tumor]), fat-containing (lipoma, liposarcoma, myelolipoma, presacral teratoma), calcified (calcified lymphocele, calcified rejected transplant kidney, rare sarcomas), or myxoid (schwannoma, plexiform neurofibroma, myxoma). Retroperitoneal leiomyomas can be distinguished from other primary retroperitoneal neoplasms on the basis of their distinguishing magnetic resonance (MR) imaging features and will be described separately.

Cystic Masses

Primary Pelvic Serous Epithelial Tumors

Primary pelvic retroperitoneal serous tumors are rare entities; to our knowledge, less than 10 cases have been reported in the literature (7–9). As its name suggests, pelvic retroperitoneal serous cystadenoma is a benign tumor, with serous cystadenocarcinoma being its malignant counterpart. Primary pelvic retroperitoneal serous tumors are most commonly seen in middle-aged (38–54-year-old) women, who may present with nonspecific symptoms including abdominal fullness, pain, fatigue, and weight loss (9,10). There is one case report of a primary pelvic retroperitoneal serous tumor in an 11-year-old girl (8).

The pathogenesis of primary retroperitoneal serous tumors is unclear, but two theories have been proposed. The first theory postulates that these tumors arise from metaplasia of coelomic epithelium; the second theory postulates that they likely arise from supernumerary and heterotopic ovarian tissue in the retroperitoneum (7,10). Documentation at surgical pathology of

RadioGraphics

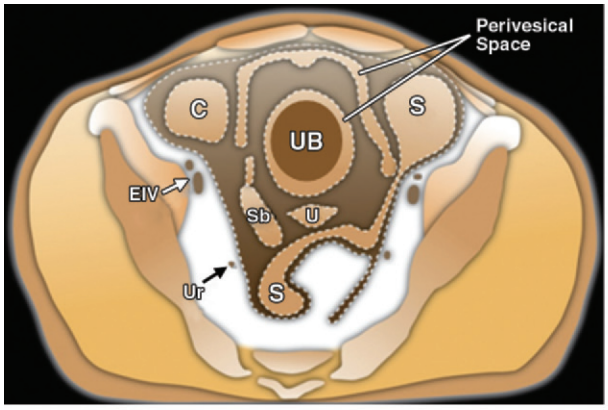

a.

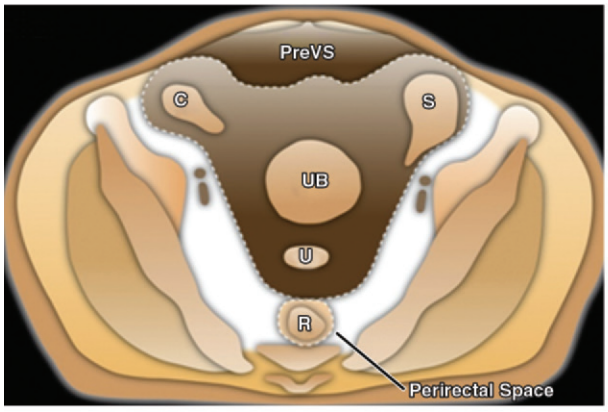

b.

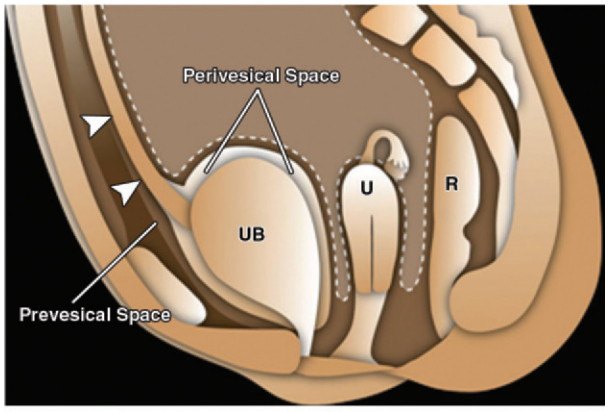

c.

Figure 1. Axial **(a, b)** and sagittal **(c)** diagrams illustrate the pelvic peritoneal reflection (dotted line in **c**) and the pelvic extraperitoneal space. The perirectal space surrounds the rectum (*R* in **b** and **c**). Arrowheads in **c** indicate the urachus with the surrounding umbilicovesical fascia, which divides the prevesical space (*PreVS* in **b**) anteriorly from the perivesical space posteriorly. *C* = cecum, *EIV* = external iliac vessels, *S* = sigmoid, *Sb* = small bowel, *U* = uterus, *UB* = urinary bladder, *Ur* = ureter.

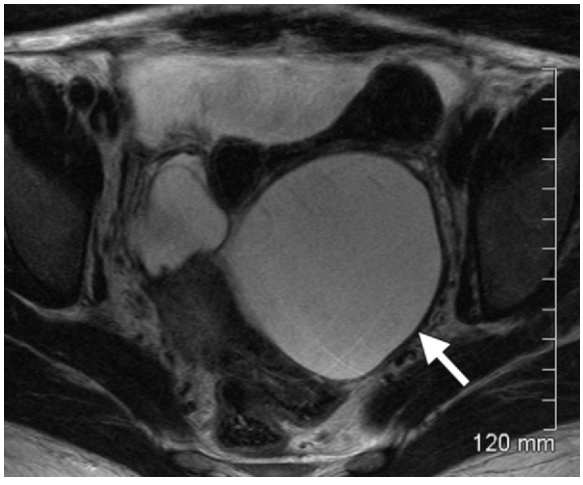

Figure 2. Serous cystadenoma. Axial T2-weighted MR image shows a well-defined, unilocular cystic lesion (arrow) in the left hemipelvis. Surgical excision was performed. Intraoperatively, the lesion was seen to be separate from the ovary and located in the retroperitoneum. Results of pathologic analysis confirmed the diagnosis of a benign serous cystadenoma.

normal ovaries that are separate and distinct from the primary mass is essential for confirming the primary retroperitoneal nature of the lesion.

At imaging, primary pelvic retroperitoneal serous tumors simulate ovarian serous tumors and appear as well-defined uni- or multiloculated cystic masses. Serous cystadenomas appear as simple cysts without solid components or mural nodularity, whereas the presence of solid components and mural nodularity raises suspicion for carcinoma. At computed tomography (CT), these tumors appear as cystic masses with enhancing mural nodules and papillary projections. Purely solid masses with areas of necrosis or calcification are uncommon. MR imaging is the optimal imaging modality for characterization of these tumors, allowing assessment of internal signal intensity as well as of the presence or absence of enhancing internal septa or mural nodularity (Figs 2, 3). The local extent of the

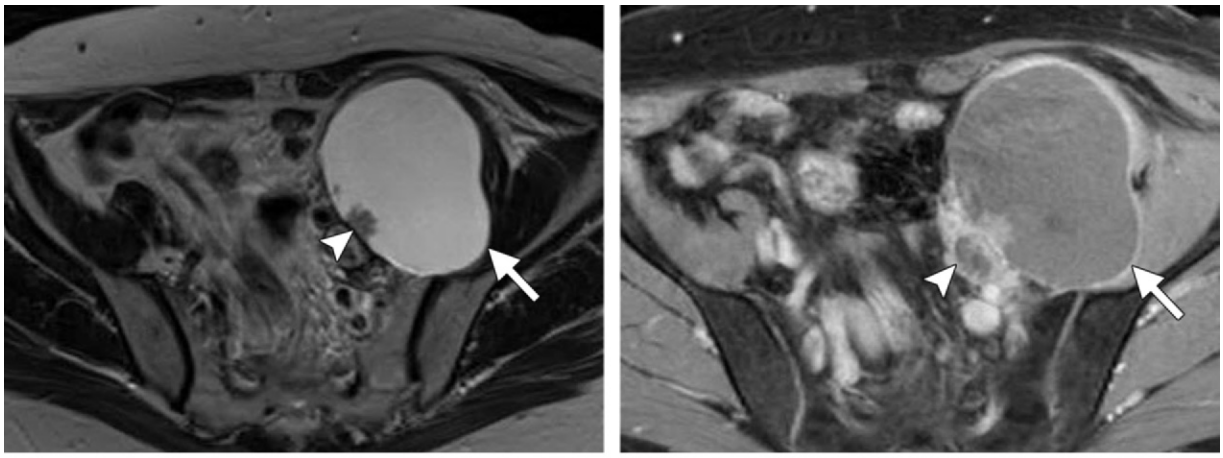

a. b.

Figure 3. Serous cystadenocarcinoma. **(a)** Axial T2-weighted MR image shows a well-defined, unilocular cystic lesion (arrow) with a solid mural nodule (arrowhead) in the left hemipelvis. **(b)** Axial contrast material–enhanced T1-weighted MR image reveals diffuse enhancement of the lesion wall (arrow) with focal heterogeneous enhancement of the mural nodule (arrowhead). Surgical excision and histopathologic analysis helped confirm the diagnosis of a primary retroperitoneal serous cystadenocarcinoma.

tumor is also better defined at MR imaging, and visualization of the normal ovaries as separate and distinct entities also reinforces the diagnosis. The lesion may insinuate posterior to a retroperitoneal structure such as the psoas muscle, a finding that confirms its retroperitoneal nature (versus the intraperitoneal growth of primary ovarian cystic neoplasms). Other imaging features that indicate a retroperitoneal location include anterior displacement of the rectum and anterior or medial displacement of the iliopsoas muscle, iliac vessels, and ureter. The differential diagnosis for retroperitoneal serous epithelial neoplasms includes other cystic retroperitoneal lesions (eg, mucinous cystadenoma or cystadenocarcinoma, lymphangioma, tailgut cyst) and intraperitoneal lesions (eg, ovarian, paraovarian, or peritoneal inclusion cyst). Ovarian lesions can be distinguished from retroperitoneal lesions in that the former usually demonstrate features such as contiguity of the lesion with the ovary, ovarian veins, or round ligament, as well as lack of visualization of the normal ovary and posterior displacement of the rectum.

Surgical excision is the treatment of choice for primary pelvic retroperitoneal serous tumors. Adjuvant or neoadjuvant chemotherapy may be necessary in some cases, as with ovarian serous cystadenocarcinoma (11). Aggressive tumors with local invasiveness, recurrences, and distant metastases have also been reported (12).

Ancient Schwannoma

Schwannomas are benign, slow-growing encapsulated tumors of nerve sheath origin. Because schwannomas typically grow slowly over a long period of time, they tend to undergo degeneration. Ancient schwannoma is a rare variant of schwannoma that is characterized by degeneration and decreased cellularity (13). It is commonly seen in elderly patients and tends to occur in the head and neck region, mediastinum, retroperitoneum, and pelvis (14–16). Ancient schwannomas in the pelvis are often asymptomatic due to their deep location and hence may be very large at presentation. Symptoms related to pressure effect and pain may be present. Histologically, ancient schwannoma is characterized by a significantly decreased Antoni type A (hypercellular) area, with the Antoni type B area occupying the majority of the tumor (13).

At imaging, ancient schwannomas appear as heterogeneously enhancing masses with cystic areas and may show calcification and, rarely, ossification. MR imaging is useful for characterizing the internal contents and defining local tumor extent. At MR imaging, ancient schwan-

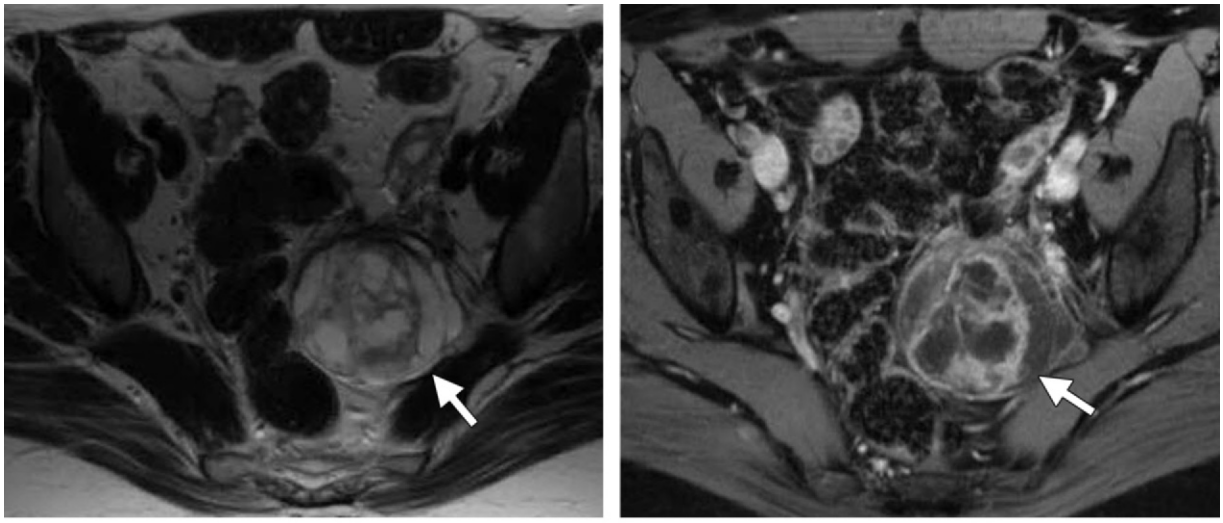

a. b.

Figure 4. Ancient schwannoma. **(a)** Axial T2-weighted MR image shows a well-defined, complex cystic lesion with internal septa and solid components (arrow) in the left hemipelvis. **(b)** Axial postcontrast T1-weighted MR image reveals heterogeneous enhancement of the internal septa and solid components (arrow). Surgical excision and histopathologic analysis helped confirm the diagnosis of ancient schwannoma.

noma appears as a well-defined, complex cystic mass with a variable enhancement pattern (Fig 4) (17). The cystic component appears as areas of low T1 and high T2 signal intensity; areas of myxoid and hemorrhagic change may also be seen within the tumor. Enhancement of the wall is commonly seen, representing the residual tumor along the circumference of the degenerating cyst or the fibrous capsule. Identification of the nerve adjacent to or along the tumor is useful for differentiating ancient schwannomas from other soft-tissue neoplasms (17). Scintigraphic studies are useful in demonstrating schwannomas and differentiating them from abscess. Schwannomas, including ancient schwannomas, show positive uptake on technetium-99m dimercaptosuccinic acid studies and do not show uptake on gallium-67 (^{67}Ga) citrate scans (17,18). The differential diagnosis for pelvic retroperitoneal ancient schwannoma includes other complex cystic lesions (eg, serous or mucinous cystadenocarcinoma), abscess, necrotic soft-tissue sarcoma, and necrotic metastatic lymphadenopathy.

The treatment of choice for ancient schwannoma is complete surgical excision, even though the majority of ancient schwannomas are benign and have a favorable outcome, with malignant transformation being extremely rare (19).

Pelvic Lymphangioma

Lymphangiomas are benign congenital tumors that arise as a result of sequestration of embryonic lymphatic vessels that have failed to communicate with the rest of the lymphatic or venous system. Lymphangiomas can be of capillary, cavernous, or cystic type (20,21). Up to 95% of lymphangiomas occur in the neck and axillary region, and most patients are children (22). Intraabdominal lymphangiomas are rarely reported in adults, and it is estimated that less than 1% of all lymphangiomas occur in the retroperitoneum (23,24), with the pelvic retroperitoneum being an even more unusual location. Pelvic lymphangiomas can occur as isolated abnormalities or as a part of congenital syndromes such as Klippel-Trénaunay-Weber syndrome (21).

Clinically, lymphangiomas are often asymptomatic but may manifest due to pressure symptoms or as a palpable mass. Presentation with acute pain or fever due to hemorrhage, rupture, or infection is rare. At CT, lymphangiomas are readily detectable as uni- or multilocular thin-walled cystic spaces (20). Calcification with lymphangioma has been described only rarely (20). At MR imaging, lymphangiomas appear as uni- or multilocular areas of low T1 and high T2

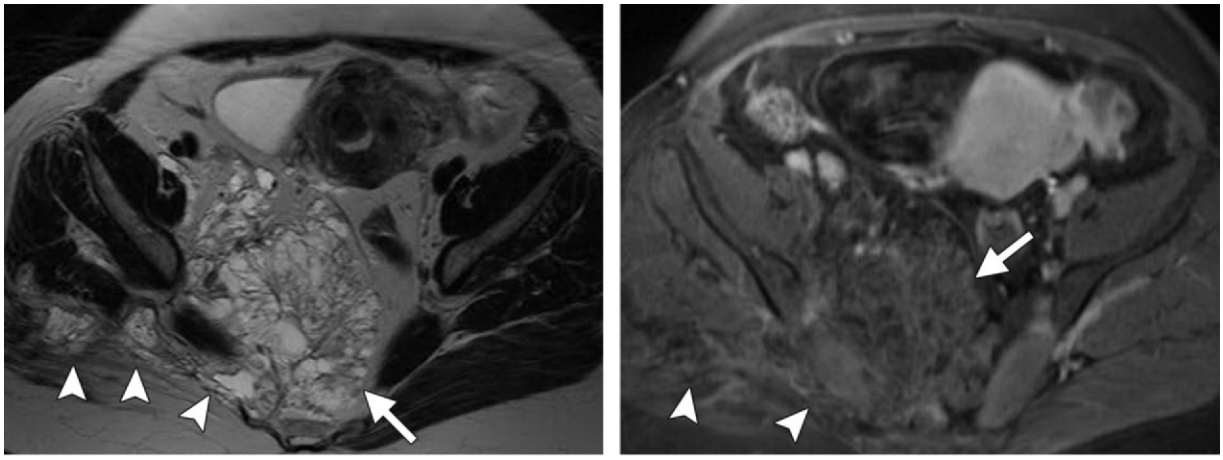

a. b.

Figure 5. Lymphangioma. **(a)** Axial T2-weighted MR image shows an ill-defined, complex cystic lesion (arrow) in the right hemipelvis. The lesion crosses the anatomic boundaries and extends along the sciatic notch into the right posterolateral gluteal region (arrowheads), a feature that is typical of lymphangioma. **(b)** On an axial postcontrast T1-weighted MR image, the lesion (arrow) demonstrates diffuse heterogeneous enhancement. Extension along the sciatic notch into the right posterolateral gluteal region (arrowheads) is again noted.

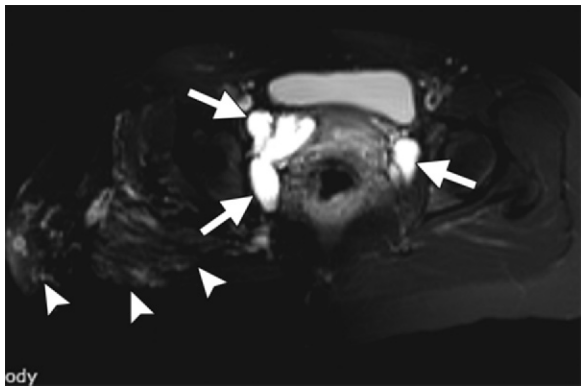

Figure 6. Multiple lymphangiomas in a patient with Klippel-Trénaunay-Weber syndrome. Axial T2-weighted MR image demonstrates multiple bilateral, well-defined hyperintense lesions (arrows) along the pelvic sidewalls (more on the right side than on the left). Asymmetric hypertrophy and prominent venous varicosities are seen in the right gluteal musculature (arrowheads), features that are typical of Klippel-Trénaunay-Weber syndrome.

signal intensity corresponding to cystic spaces with thin, almost imperceptible walls. No significant enhancement is seen following the administration of gadolinium-based contrast material (Figs 5, 6). MR imaging is useful for differentiating lymphangiomas from other cystic masses or neoplasms in the pelvic retroperitoneum such as serous or mucinous epithelial neoplasms, tailgut cyst, peritoneal inclusion cyst, or ancient schwannoma. One of the characteristic imaging features of lymphangioma that helps differentiate it from other cystic pelvic masses is its ability to cross from one compartment to another, reflecting the pathway of developing lymphatic vessels (20).

Tailgut Cyst

Tailgut cysts, or retrorectal cystic hamartomas, arise from incomplete regression of a portion of the gut distal to the as yet undeveloped anus. They are most commonly seen in middle-aged women but may manifest at any age (25). Most tailgut cysts are discovered incidentally, but symptoms of rectal or perineal pain, painless rectal bleeding, and increased urinary frequency may be present (26,27). Secondary infection of the cyst may cause fever and acute pelvic pain. Malignant degeneration is rarely seen, with adenocarcinoma being the most common malignancy within a tailgut cyst (28). Carcinoid tumors, neuroendocrine tumors, and sarcomas have also been described in association with tailgut cysts (28,29).

At imaging, tailgut cysts appear as well-defined, thin-walled uni- or multilocular cystic lesions in the perirectal space without any internal enhance-

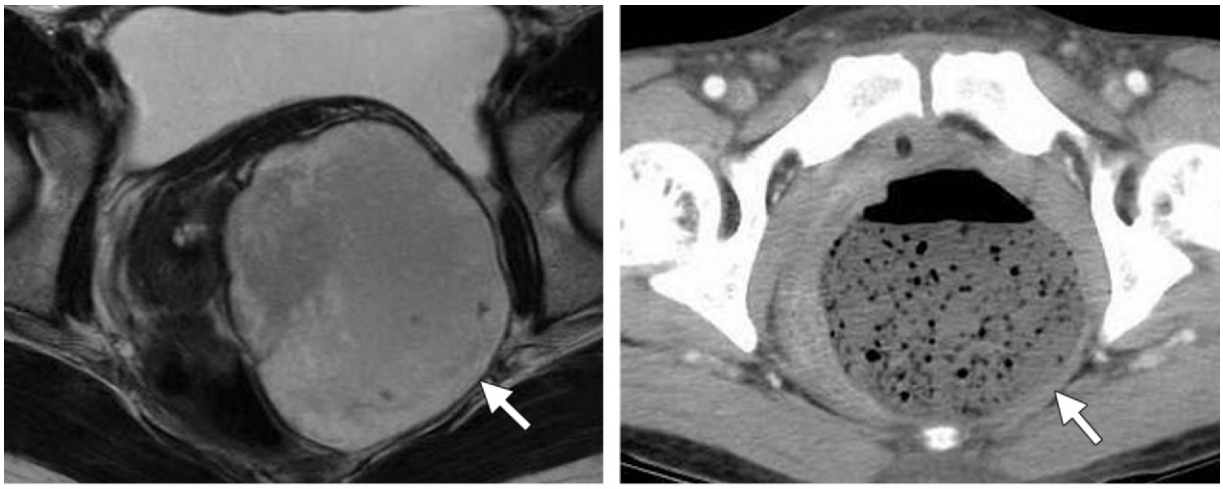

a. b.

Figure 7. Tailgut cyst. **(a)** Axial T2-weighted MR image shows a large, hyperintense, unilocular cystic lesion in the left hemipelvis (arrow). No solid components are seen. At T1-weighted imaging, the lesion was hypointense with a thin enhancing wall. **(b)** On a follow-up axial contrast-enhanced CT scan obtained 3 months later, the lesion contains an air-fluid level and has a thick enhancing wall (arrow), findings that are consistent with secondary infection.

ment. At MR imaging, they appear as well-marginated thin-walled lesions with low to intermediate T1 signal intensity and high T2 signal intensity (Fig 7). An uncomplicated cyst usually has a thin wall, which may show mild enhancement (26). The presence of a thick enhancing wall with or without surrounding inflammation or an air-fluid level suggests secondary infection. The presence of asymmetric irregular wall thickening with heterogeneous enhancement following contrast material administration raises suspicion for malignant change within a duplication cyst (28).

Teaching Point

Given their malignant potential, it is important that tailgut cysts be differentiated from other cystic lesions in this location, such as epidermoid or dermoid cyst, rectal duplication cyst, anterior meningocele, and cystic lymphangioma. Cystic lymphangioma and tailgut cysts are often multilocular, whereas the rest of the aforementioned cystic lesions are commonly unilocular. Complete surgical excision is the treatment of choice for tailgut cysts.

Vascular or Hypervascular Masses

Pelvic SFT

SFT is a ubiquitous neoplasm of fibroblastic cell origin that was initially thought to be confined to the pleural surface. Extrapleural SFTs are now considered to be more common. SFTs in the pelvis may arise from the pelvic peritoneum or in the retroperitoneum. Pelvic SFTs are commonly seen in the 5th decade of life (age range, 20–70 years) and do not exhibit any gender predilection (30). They are usually benign, and, although malignant degeneration has been reported, its exact incidence is unknown. Because of their deep location, most pelvic SFTs remain asymptomatic, although a small number of patients may present with pressure symptoms. Hypoglycemia is a rare paraneoplastic manifestation of SFT that is seen in less than 5% of cases (31).

Teaching Point

At imaging, SFTs appear as well-defined masses with intense heterogeneous enhancement that persists on delayed phase images obtained following contrast material administration. Areas of central low attenuation representing necrosis, hemorrhage, or cystic change may be seen. Calcification arising within an SFT is rare and is usually seen in large tumors. Typical MR imaging findings include intermediate T1 signal intensity and heterogeneous T2 signal intensity, with multiple flow voids representing prominent vascular channels on T2-weighted images. Intense arterial enhancement is also seen and indicates the hypervascular nature of the mass (Fig 8) (32). Persistent delayed enhancement may be encountered, a finding that suggests the fibrous component of the tumor. The

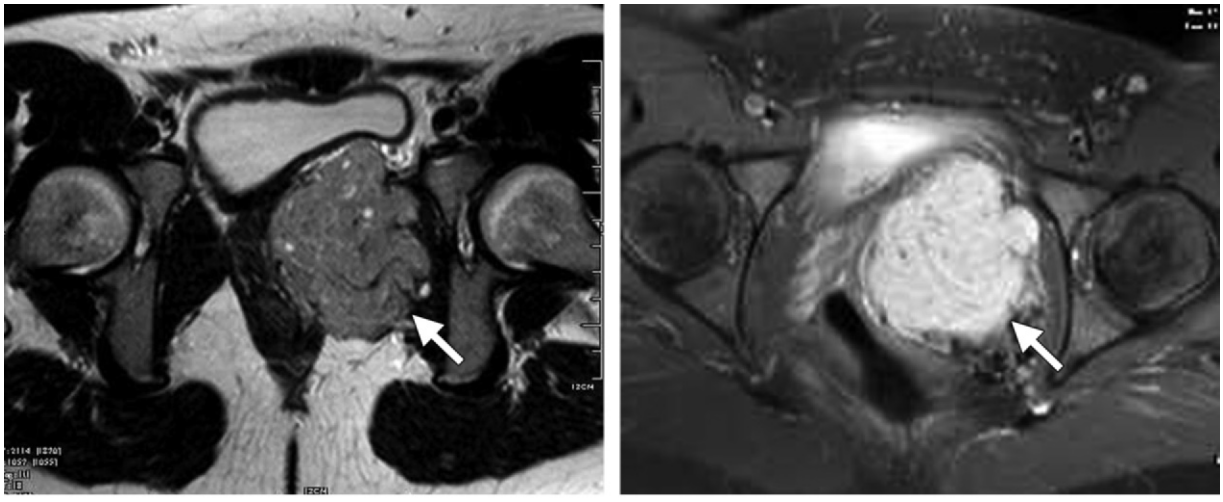

a. b.

Figure 8. Pelvic SFT. **(a)** Axial T2-weighted MR image shows a well-defined lobulated lesion (arrow) in the left hemipelvis. **(b)** On an axial MR image obtained following the administration of gadolinium-based contrast material, the lesion (arrow) shows intense heterogeneous enhancement. Surgical excision and histopathologic analysis helped confirm the diagnosis of an SFT.

differential diagnosis includes other hypervascular neoplasms (eg, angiosarcoma, hemangioendothelioma, angiomyxoma) and fibrous neoplasms (eg, malignant fibrous histiocytoma, fibrosarcoma, leiomyoma, desmoid tumor).

Complete surgical resection is the treatment of choice for pelvic SFT (33). Preoperative embolization can reduce intraoperative hemorrhage. In unresectable disease, surgical cytoreduction with intraoperative chemotherapy and radiation therapy has been found to be useful (34). Local recurrences occur only rarely but have been reported up to 20 months after the initial diagnosis of malignant pelvic SFT, thereby necessitating long-term follow-up (35).

Extraadrenal Pheochromocytoma or Paraganglioma

Pheochromocytoma is a neuroendocrine tumor composed of chromaffin cells arising from the adrenal gland. The term *paraganglioma* refers to tumors arising from extraadrenal chromaffin tissue (paraganglion cells) and can occur in the retroperitoneum (including the organ of Zuckerkandl), the head and neck region, and the urinary bladder. Paraganglioma of the organ of Zuckerkandl can manifest as a pelvic retroperitoneal mass and was first described in 1902; since that time, about 135 cases have been reported in the literature (36). This disease entity is most commonly seen in men between 20 and 40 years of age and is functional with associated hypertension in over three-fourths of cases (36). Nonfunctional tumors may manifest with abdominal pain or a mass (36). Unlike adrenal pheochromocytomas, approximately 30%–40% of extraadrenal pheochromocytomas are malignant (37). Paragangliomas can occur in isolation or as a part of multisytemic disorders such as multiple endocrine neoplasia type 2a, neurofibromatosis, von Hippel–Lindau disease, or the triad of Carney (gastric leiomyosarcoma, pulmonary chondroma, and extraadrenal paraganglioma) (38).

At CT, paraganglioma appears as a well-defined hypervascular mass in the pelvic retroperitoneum along the course of the common iliac vessels. These tumors may be heterogeneous with foci of calcification. Evidence of local invasion and metastasis may be seen in malignant tumors. At MR imaging, pheochromocytoma appears as areas of low T1 and high T2 signal intensity and shows avid enhancement following the administration of gadolinium-based contrast material (Fig 9) (38). The sensitivity of CT and MR imaging for the detection of extraadrenal pheochromocytoma is approximately 90% (38). MIBG scintigraphy has traditionally been used to localize adrenal pheochromocytoma as well as extraadrenal paraganglioma. MIBG scintigraphy with iodine-123

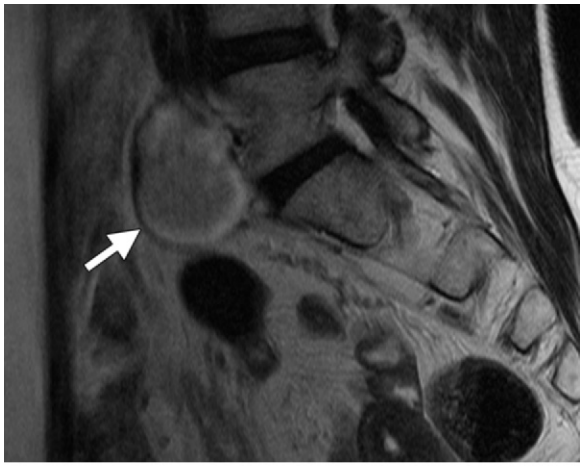

a.

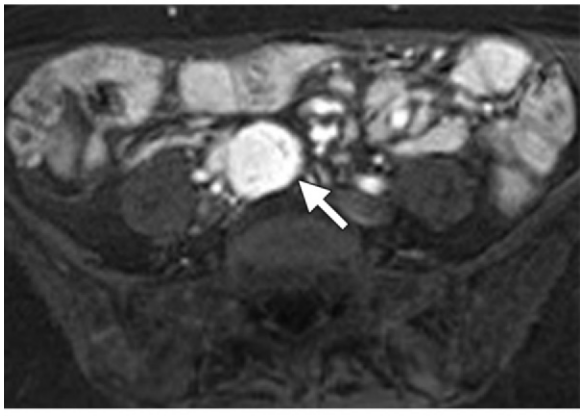

b.

Figure 9. Extraadrenal pheochromocytoma-paraganglioma. Sagittal T2-weighted **(a)** and axial gadolinium-enhanced T1-weighted **(b)** MR images demonstrate a lesion (arrow) with T2 hyperintensity and intense contrast enhancement, imaging features that are typical of extraadrenal pheochromocytoma-paraganglioma. Metaiodobenzylguanidine (MIBG) scintigraphy showed intense uptake within the lesion, confirming the diagnosis.

(^{123}I) or ^{131}I is fairly sensitive (77%–95%) but highly specific (95%–100%) for the detection of pheochromocytoma or paraganglioma (38,39). Indium-111 (^{111}In) pentetreotide scintigraphy has a high sensitivity (up to 94%) for the detection of paraganglioma, especially for lesions larger than 1.5 cm (40). Recently, fluorine-18 (^{18}F)–fluorodihydroxyphenylalanine positron emission tomography has been shown to be superior to ^{123}I MIBG scintigraphy in the detection of extraadrenal paragangliomas (especially the predominantly noradrenaline-secreting and hereditary types), with an overall sensitivity and specificity of up to 98% and 100%, respectively (41).

The differential diagnosis for paraganglioma in the pelvic retroperitoneum includes nerve sheath tumors, hypervascular lymphadenopathy (metastases or Castleman disease), and other hypervascular soft-tissue sarcomas. Symptoms of excess catecholamine production, as well as elevated urine vanillylmandelic acid levels and serum and urine norepinephrine levels, are highly diagnostic for paraganglioma (42). Percutaneous biopsy of a hypervascular pelvic retroperitoneal mass without adequate laboratory evaluation and prebiopsy preparation (such as pharmacologic blockade) should be avoided, since it can result in hypertensive crisis or even death.

Congenital Pelvic AVM

Congenital AVMs represent undifferentiated vascular structures that arise due to arrested vascular embryonic development. Congenital AVMs are uncommon and are usually located in the extremities, neck, and face (43). Pelvic AVMs are usually acquired and only rarely congenital. Clinically, pelvic AVMs are indolent, have a long latency period before presentation, and usually manifest with chronic vague symptoms. Pelvic pain, vaginal bleeding, hematuria, and a pulsatile mass are some of the most commonly described symptoms of pelvic AVM (44,45). As with AVMs in other locations, high-output congestive heart failure can also be seen with pelvic AVMs.

Teaching Point

MR imaging is the noninvasive imaging modality of choice for the diagnosis of pelvic AVMs and the delineation of their size and extent (46). The anatomic details seen at MR imaging (including the relationship of AVMs to adjacent pelvic structures) help in preoperative evaluation and preembolization planning. However, digital subtraction angiography of the iliac arteries is the standard of reference. AVMs appear as flow voids on T1- and T2-weighted MR images; contrast-enhanced MR imaging and conventional angiography usually show multiple tortuous feeding vessels from the iliac artery (Fig 10) (46). Management of congenital pelvic AVMs depends on their location and the patient's symptoms and includes complete surgical resection, embolization, or surgical ligation of the feeding vessels. In contrast, asymptomatic pelvic AVMs are usually managed conservatively with careful clinical and imaging surveillance (47).

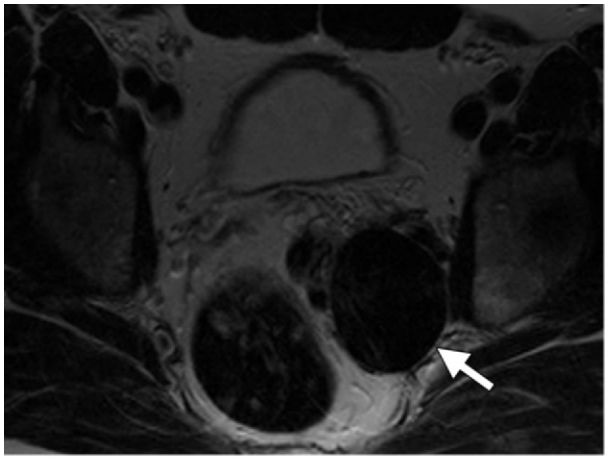

a.

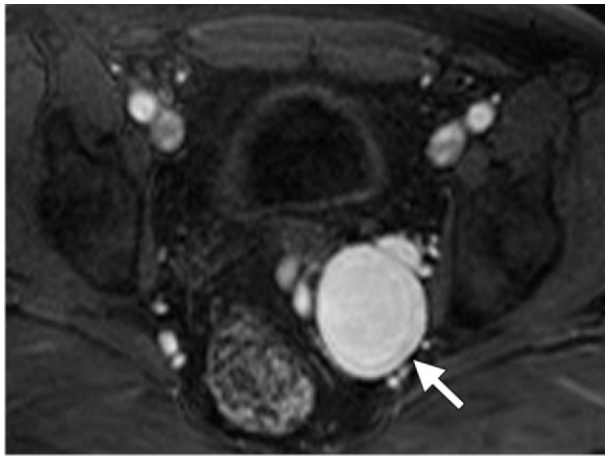

b.

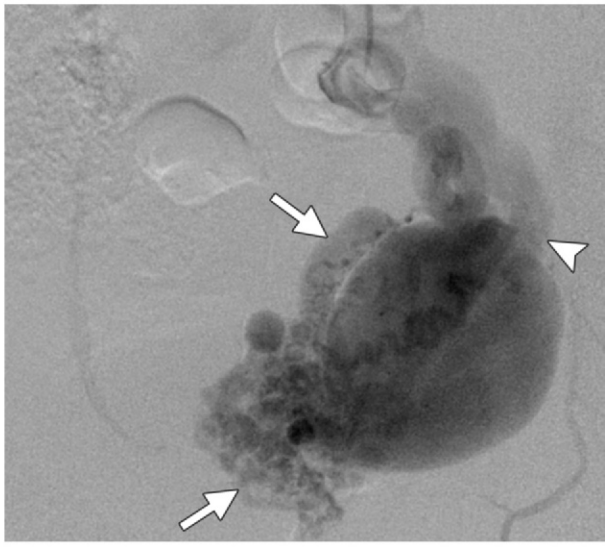

c.

Figure 10. Congenital pelvic AVM. **(a, b)** Axial T2-weighted **(a)** and gadolinium-enhanced T1-weighted **(b)** MR images reveal a lesion in the left hemipelvis (arrow) that is T2 hypointense and enhances intensely after contrast material administration. The proximity of the lesion to the internal iliac artery as well as its signal intensity characteristics raised suspicion for a vascular malformation. **(c)** Digital subtraction angiogram obtained after contrast material injection shows multiple dilated tortuous feeding vessels from the internal iliac artery (arrows) with early opacification of the iliac vein (arrowhead), findings that are consistent with an AVM.

Klippel-Trénaunay-Weber Syndrome

Klippel-Trénaunay-Weber syndrome consists of the triad of capillary malformations, soft-tissue or bone hypertrophy, and venous varicosities or malformations (48). The abnormality primarily involves the extremities (lower extremity in nearly 95% of cases), with only rare involvement of the thoracic, abdominal, and pelvic regions (49). Klippel-Trénaunay-Weber syndrome is generally sporadic with an equal gender distribution. Although Klippel-Trénaunay-Weber syndrome typically manifests at birth, initial manifestation in late childhood or adolescence is not uncommon. Venous varicosities may be seen in the pelvic retroperitoneum in contiguity with involvement of the genitalia, with or without involvement of the limbs. Lymphatic abnormalities are seen in the majority of patients with Klippel-Trénaunay-Weber syndrome and include lymphangitis and cutaneous lymphatic vesicles as well as micro- and macrocystic lymphatic malformations in the abdomen (50).

At imaging, the extensive venous varicosities and cystic lymphatic malformations may both be seen in the pelvic retroperitoneum (Fig 11). The presence of multiple phleboliths throughout the pelvic retroperitoneum at multidetector CT confirms the presence of vascular malformations or venous varicosities.

Primary Pelvic Retroperitoneal GIST

GISTs are rare mesenchymal neoplasms of the gastrointestinal tract. Rarely, they can arise in extraintestinal locations, including the mesentery, omentum, and retroperitoneum (51). The pelvic retroperitoneum is an extremely rare location for GISTs. Extraintestinal GISTs resemble intestinal GISTs histologically and immunophe-

RadioGraphics

Figure 11. Klippel-Trénaunay-Weber syndrome. Axial T2-weighted MR image **(a)** and unenhanced CT scan **(b)** reveal innumerable T2 hyperintense lesions throughout the pelvis (arrows in **a**) with multiple phleboliths (arrows in **b**), findings that are consistent with extensive venous varicosities. Prominent venous varicosities are also seen in the right gluteal region (arrowhead in **a**).

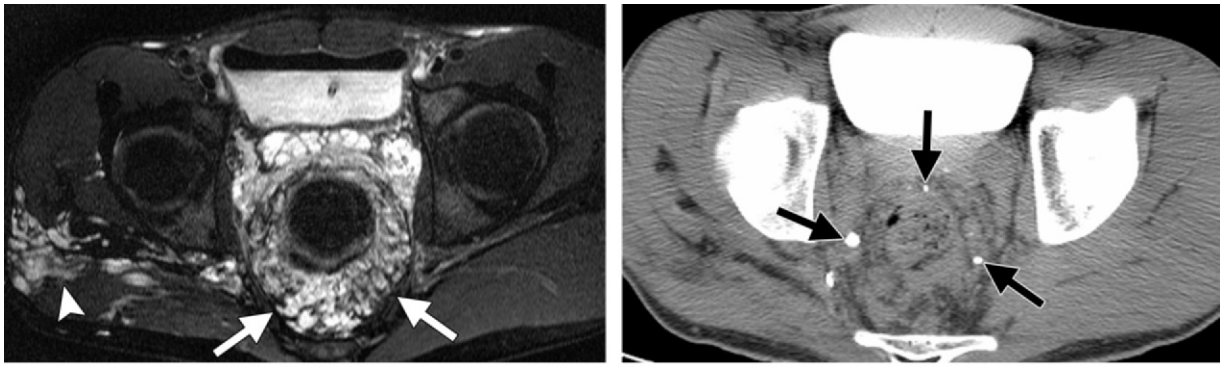

a. **b.**

Figure 12. GIST. **(a)** Sagittal T2-weighted MR image shows a large mass in the left hemipelvis (arrow) containing multiple areas of low signal intensity. **(b)** On an axial gadolinium-enhanced T1-weighted MR image, the mass (arrows) shows moderate heterogeneous enhancement. *U* = uterus. Surgical excision and histopathologic analysis helped confirm the diagnosis of a benign GIST.

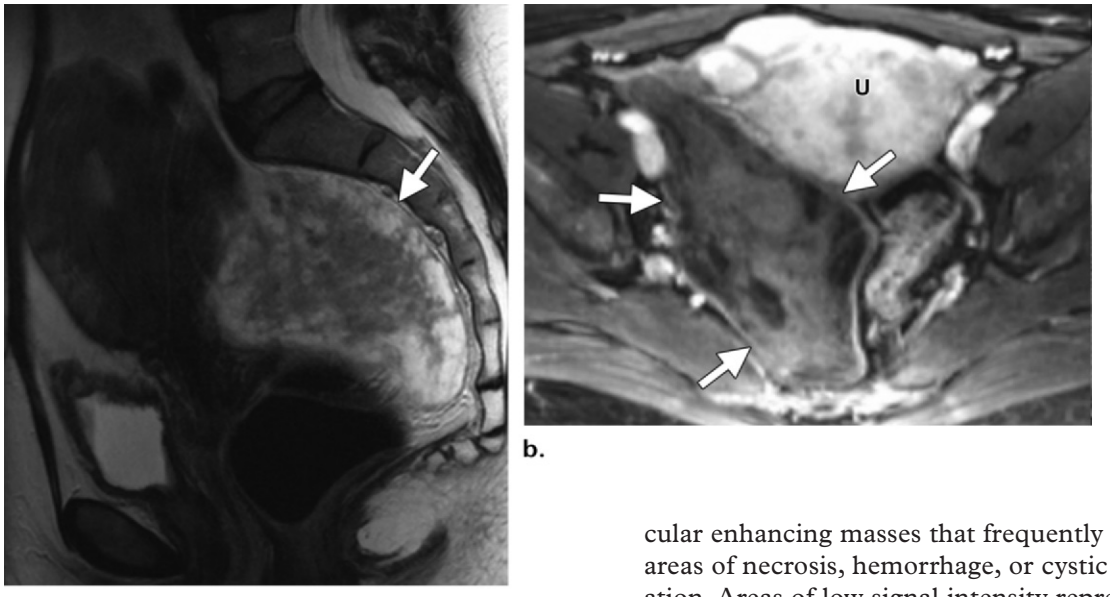

a. **b.**

notypically; however, they tend to be aggressive, with a higher rate of malignancy (51). In the largest series to date of patients with extraintestinal GISTS (n = 48), these tumors occurred over a wide age range (31–82 years) and were more common in women (female-to-male ratio, 2:1). At imaging, they appear as large, hypervascular enhancing masses that frequently harbor areas of necrosis, hemorrhage, or cystic degeneration. Areas of low signal intensity representing fibrosis may be seen on T2-weighted MR images (Fig 12). Given the rarity of primary pelvic retroperitoneal GISTs, biopsy or surgical excision and histopathologic analysis are mandatory for the diagnosis; differentiation from other hypervascular soft-tissue tumors is not possible solely on the basis of clinical and imaging features.

Fat-containing Masses

Pelvic Retroperitoneal Lipoma or Liposarcoma

Lipoma is a benign mesenchymal tumor composed of mature adipose tissue, whereas liposarcoma is its malignant counterpart. These tumors can be encountered virtually anywhere in the body at any age. Primary pelvic liposarcomas as well as retroperitoneal liposarcomas extending into the pelvis may mimic gynecologic disease (52,53). Retroperitoneal and pelvic liposarcomas can be asymptomatic for a long period of time and commonly manifest in elderly patients (5th–7th decades of life) (54,55).

At CT, lipomas appear as well-defined homogeneous masses with fat attenuation. Areas of soft-tissue attenuation may be seen within the tumor and may represent fat necrosis, septa, or normal adjacent structures. However, the presence of a predominantly solid soft-tissue component or adjacent organ invasion should raise suspicion for liposarcoma. The imaging appearance of liposarcoma varies depending on the tumor grade. Well-differentiated liposarcomas appear as well-defined, predominantly fat-containing lesions with minimal soft-tissue attenuation, whereas poorly differentiated tumors appear as locally invasive, predominantly soft-tissue masses with minimal fat (Fig 13) (55).

Figure 13. Liposarcoma. Axial contrast-enhanced CT scan shows a well-defined soft-tissue lesion (arrow) with areas of low attenuation (inset). Surgical excision and histopathologic analysis helped confirm the diagnosis of a well-differentiated liposarcoma.

Presacral Myelolipoma

Myelolipoma is a benign tumor that consists of mature adipose tissue and normal hematopoietic components. More than 85% of myelolipomas originate in the adrenal glands. Presacral myelolipomas account for up to 50% of all extraadrenal myelolipomas and occur predominantly in elderly women (average age, 65 years; female-to-male ratio, 2:1) (56,57). Presacral myelolipomas are usually asymptomatic but may manifest with pressure symptoms due to mass effect on the rectum, ureters, or urinary bladder. The association of myelolipomas with Cushing syndrome, Addison disease, and exogenous steroid use has been reported (57).

At CT, presacral myelolipomas appear as well-circumscribed, predominantly fat-containing masses that contain areas of soft-tissue attenuation. At MR imaging, areas of high T1 signal intensity and intermediate to high T2 signal intensity with loss of signal intensity on fat-suppressed images are characteristic and confirm the presence of intratumoral fat (Fig 14). The tumors may be large at presentation and range from 5 to 19 cm in size. Presacral myelolipomas show variable enhancement. Areas of intratumoral hemorrhage or calcification may also be seen.

The differential diagnosis for fat-containing presacral masses includes lipoma, liposarcoma, teratoma, and lipomatosis. Liposarcoma typically exhibits infiltrative growth, unlike the well-encapsulated myelolipoma. Teratoma is usually seen in younger individuals, whereas myelolipoma is typically seen in elderly patients. The differentiation of presacral myelolipoma from other fat-containing lesions may not always be possible with imaging alone. The fact that presacral myelolipoma occurs predominantly in elderly women is the single most distinguishing feature that helps differentiate this tumor from other fat-containing presacral lesions.

Teaching Point

Presacral Teratoma

Teratoma is a germ cell tumor composed of elements from more than one germ cell layer. Presacral teratomas are commonly seen in infants and children, with a prevalence of approximately one in every 40,000 live births (58). About 100 cases of presacral teratoma in adults have been reported, with women being affected more often than men (female-to-male ratio, 4:1) (58,59).

Clinically, presacral teratomas may be asymptomatic or may manifest with a mass, recurrent pilonidal infections, or pressure symptoms, including constipation (59). At imaging, presacral teratomas may have varied appearances ranging from cystic to solid; areas of intratumoral fat may also be seen (Fig 15). Benign tumors in adults

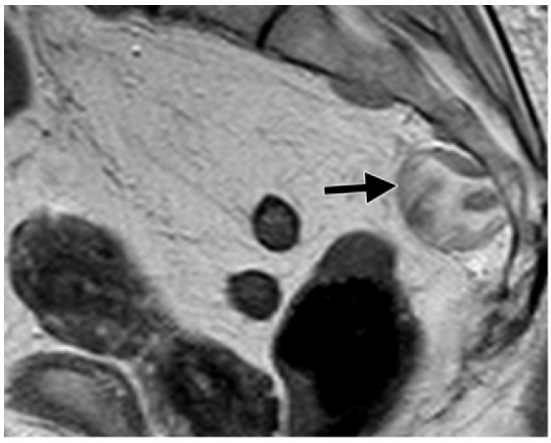

a.

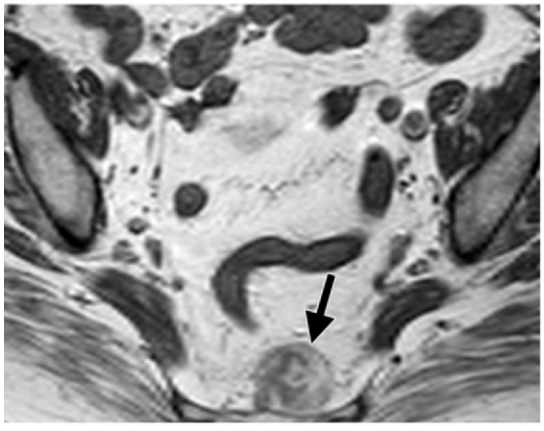

b.

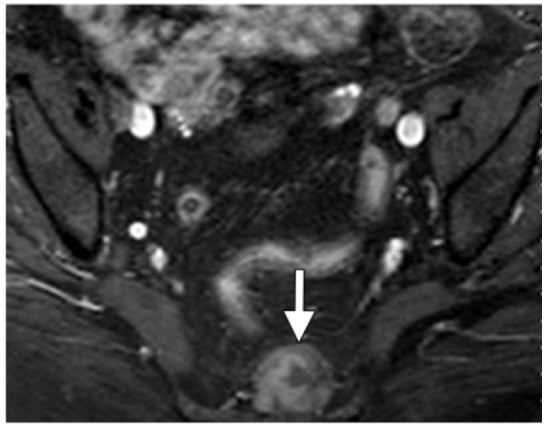

c.

Figure 14. Presacral myelolipoma in an 85-year-old woman. **(a, b)** Sagittal T2-weighted **(a)** and axial non-fat-suppressed T1-weighted **(b)** MR images reveal a well-defined hyperintense lesion (arrow) in the presacral space. **(c)** Axial gadolinium-enhanced fat-suppressed T1-weighted MR image shows the lesion (arrow) with moderate heterogeneous enhancement and areas of signal intensity loss that represent macroscopic fat. Results of percutaneous CT-guided biopsy confirmed the diagnosis of myelolipoma.

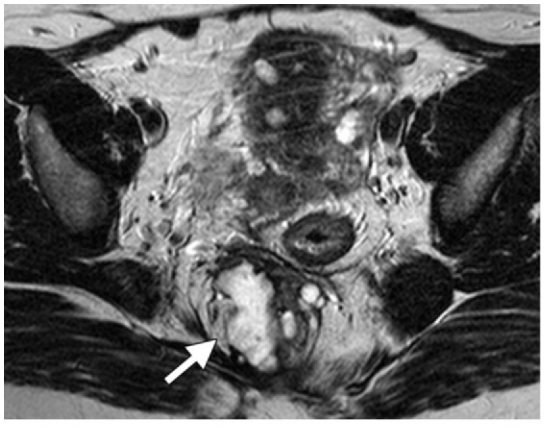

a.

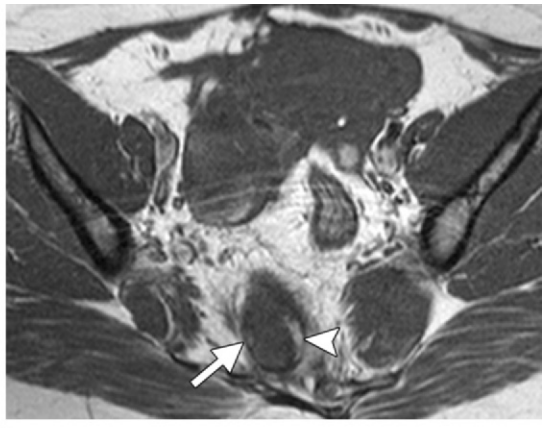

b.

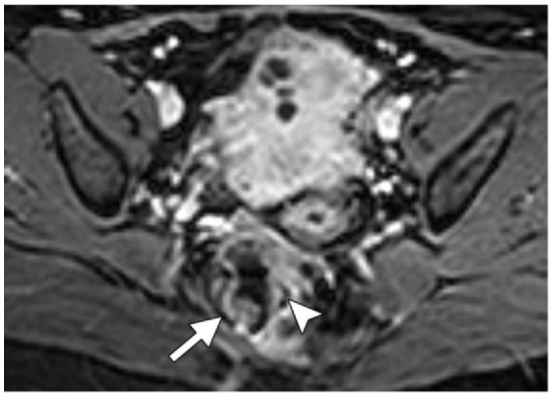

c.

Figure 15. Presacral teratoma with malignant degeneration. **(a)** Axial T2-weighted MR image shows an ill-defined, heterogeneously hyperintense lesion (arrow) in the presacral space. **(b, c)** On non-fat-suppressed **(b)** and gadolinium-enhanced fat-suppressed **(c)** T1-weighted MR images, the lesion (arrow) is isointense with focal hyperintense areas. Moderate heterogeneous enhancement is seen on the gadolinium-enhanced image. Arrowhead indicates macroscopic fat. Surgical excision helped confirm the diagnosis of malignancy within a presacral teratoma.

Figure 16. Calcified lymphocele in a patient with a history of renal transplantation. Axial unenhanced CT scan through the pelvis reveals a well-defined cystic lesion with uniform thick calcification of the wall (arrow). CT performed 4 years earlier did not show any wall calcification. However, the lesion remained stable in size over the intervening 4 years.

Figure 17. Calcified pelvic transplant kidney in a patient with a history of chronic rejection of renal transplant. Axial contrast-enhanced CT scan shows an atrophic kidney with multiple foci of calcification (arrow). A linear soft-tissue area extending from the kidney to the external iliac vessels (arrowhead) represents thrombosed, nonopacified residual transplant vasculature and confirms that the mass is a calcified renal transplant.

may or may not involve the bone (sacrum). Up to 10% of presacral teratomas may be malignant, and tumors in adults are more likely to be malignant than tumors in children. Because benign and malignant tissues can coexist within a presacral teratoma, surgical excision and careful histopathologic analysis are necessary to exclude malignancy in all adult patients (59).

Calcified Masses

Lymphocele or Rejected Transplant Kidney

Lymphoceles are fluid-filled cysts that occur secondary to injury to lymphatic vessels, commonly after lymphadenectomy or renal transplant surgery in the pelvis. Up to 30% of patients undergoing lymphadenectomy, and up to 18% of patients undergoing renal transplantation, may develop lymphocele (60). Small, sterile lymphoceles are usually asymptomatic; in symptomatic lymphoceles, symptoms may arise due to pressure effect from large size (abdominal distention, pain, constipation, or limb edema) or secondary infection (60). At CT, lymphoceles are seen as well-defined cystic lesions with a thin wall. Long-standing lymphoceles may rarely show wall calcification (Fig 16).

Chronically rejected transplant kidney can calcify, thereby simulating a calcified pelvic ret-

a. b.

Figure 18. Uncommon pelvic retroperitoneal sarcomas with calcification. **(a)** Axial contrast-enhanced CT scan obtained in a patient with pleomorphic spindle cell carcinoma shows a pelvic retroperitoneal mass with calcification (arrows). **(b)** Axial contrast-enhanced CT scan obtained in a patient with an osteoclastic giant cell sarcoma shows a large, right hemipelvic retroperitoneal mass (arrows) with foci of calcification (arrowheads).

roperitoneal mass (Fig 17). A history of renal transplantation and the presence of vascular anastomosis in the pelvis are the major clues to this diagnosis when a calcified pelvic mass is encountered.

Primary Pelvic Retroperitoneal Sarcoma

The retroperitoneum is a common location of soft-tissue sarcomas. Certain types of sarcomas may demonstrate calcification, including malignant fibrous histiocytoma (or undifferentiated pleomorphic sarcoma), synovial sarcoma (in up to 30% of cases), dedifferentiated liposarcoma, extraskeletal osteosarcoma, and other spindle cell sarcomas (Fig 18). Sarcoma should be considered a likely diagnosis when a large, heterogeneous pelvic retroperitoneal mass with local invasion is encountered. Other rare, benign neoplastic causes of calcified masses in the pelvic retroperitoneum include ganglioneuroma, schwannoma, paraganglioma, hemangioma, and presacral teratoma (61).

Myxoid Masses

Myxoma

Myxoma is a benign mesenchymal neoplasm that is thought to originate from defective differentiation of primitive mesenchymal cells into abnormal fibroblasts (62). The abnormal fibroblasts produce excessive mucopolysaccharide and immature collagen fibers, resulting in the typical histologic appearance of stellate cells and reticulin fibers in the background of myxoid stroma (63). Myxomas can occur in various anatomic locations, including the heart (atrial myxomas) and somatic soft tissues (bone, muscle, skin, and subcutaneous tissue), as well as the gastrointestinal and genitourinary tracts (64). Most noncardiac myxomas are intramuscular myxomas of the lower extremity (65). Primary retroperitoneal or pelvic myxomas are rare. Soft-tissue myxomas can manifest over a wide age range; the majority occur in the 5th decade of life, with a female

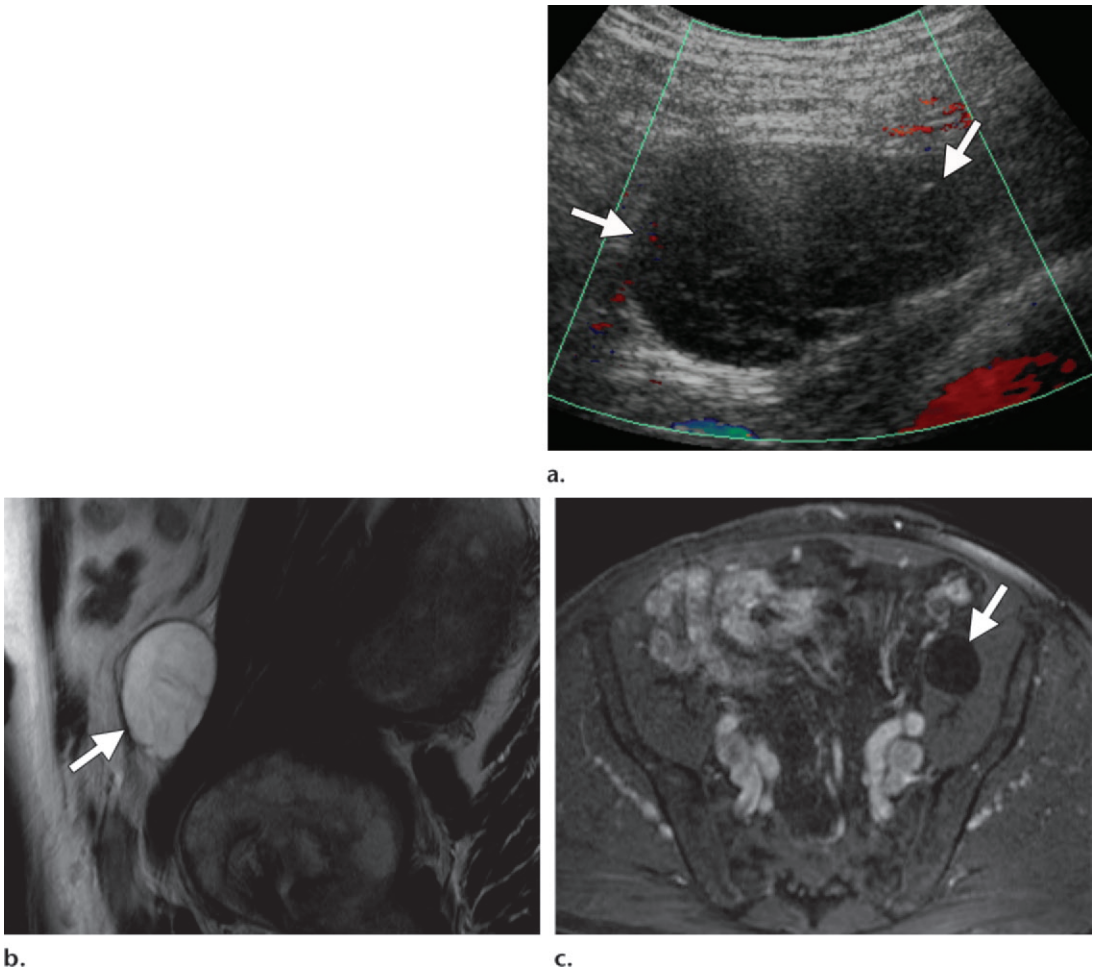

Figure 19. Intermuscular myxoma. **(a)** Color Doppler US image shows a hypoechoic mass with multiple internal septa (arrows) along the pelvic sidewall. **(b)** Sagittal T2-weighted MR image shows a hyperintense lesion (arrow) in the left hemipelvis anterior to the iliopsoas muscle. Note the fine linear regions of hypointensity within the lesion. **(c)** Axial gadolinium-enhanced T1-weighted MR image shows the lesion with minimal heterogeneous enhancement (arrow). The lesion proved to be a myxoma at histopathologic analysis.

predilection (65). A slow-growing painless mass is the most common clinical manifestation. Multiple myxomatous lesions are seen in patients with Albright syndrome.

Pathologically, myxomas are composed of spindle cells and stellate cells in an abundant myxoid background. At ultrasonography (US), myxomas appear as solid hypoechoic lesions. Cystic spaces and multiple internal septa may also be seen. At CT, myxomas appear as well-defined low-attenuation lesions with variable heterogeneous enhancement. At MR imaging, they manifest as well-circumscribed lesions with uniformly low T1 and high T2 signal intensity, with variable heterogeneous enhancement following the administration of gadolinium-based contrast material (Fig 19) (65). Areas of cystic change can be seen within the tumor as nonenhancing areas at contrast-enhanced CT or MR imaging (65).

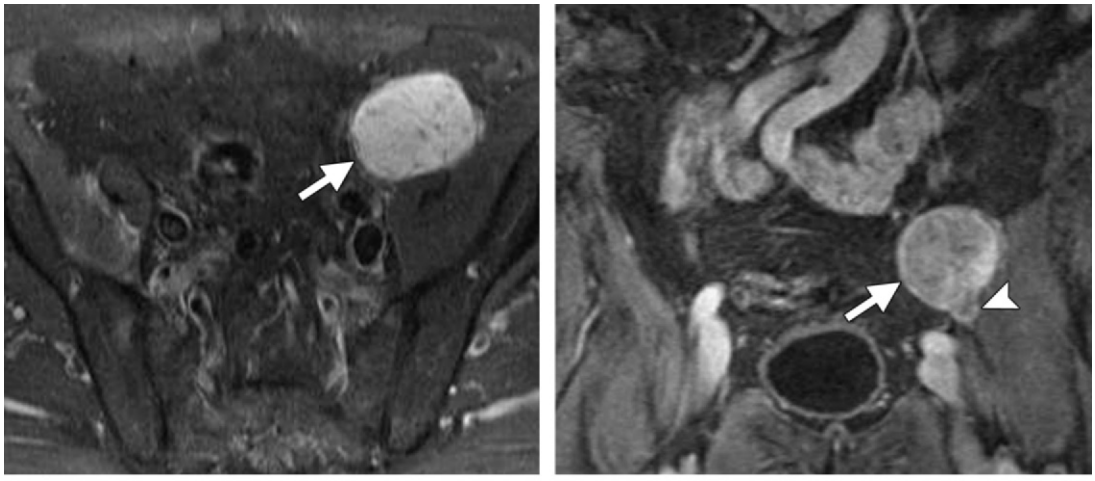

a. b.

Figure 20. Schwannoma. **(a)** Axial T2-weighted MR image shows a homogeneously hyperintense lesion (arrow) in the left hemipelvis. **(b)** Coronal gadolinium-enhanced T1-weighted MR image shows the lesion with moderate homogeneous enhancement (arrow). Arrowhead indicates nodular extension of the mass along the expected course of the nerve. On the basis of these findings, a diagnosis of neurogenic tumor was made. Results of percutaneous biopsy confirmed the lesion to be a schwannoma.

The radiologic differential diagnosis for pelvic retroperitoneal myxomas includes synovial cyst, bursa, ganglion, neurogenic tumor, and myxoid sarcoma, the first three of which most commonly occur in the dorsum of the wrist and the popliteal region and are rare in the pelvis (65). However, a migrated iliopsoas bursa can manifest as a cystic lesion in close relation to the iliopsoas muscle in the pelvis. Myxomas can be differentiated from these purely cystic lesions based on the presence of *(a)* internal echoes and lack of increased through transmission at US, and *(b)* contrast enhancement at CT and MR imaging. Neurogenic tumors are more common and can be distinguished on the basis of their typical targetlike appearance and their contiguity with the nerve (66).

Primary Pelvic Retroperitoneal Schwannoma

Schwannoma is a benign neurogenic tumor of nerve sheath origin that is commonly seen in the head, neck, and extremities. Schwannomas account for up to 6% of all retroperitoneal tumors and may occur in paravertebral, perirenal, or presacral pelvic retroperitoneal locations (67–69). They are commonly seen in young to middle-aged females (female-to-male ratio, 2:1) (70). Retroperitoneal schwannomas are usually asymptomatic and incidentally detected and may be unusually large at presentation (68).

Schwannomas manifest as well-defined hypoechoic masses at US and as hypoattenuating masses at CT. Areas of cystic degeneration, calcification, or hemorrhage may also be seen at CT. At MR imaging, schwannomas appear as well-defined masses with heterogeneous low signal intensity on T1-weighted images and high signal intensity on T2-weighted images (Fig 20). A targetlike pattern consisting of peripheral high signal intensity (representing Antoni B areas) and central low signal intensity (representing Antoni A areas) may also be seen on T2-weighted images. Contrast enhancement varies depending on cellularity and the presence of degenerative change. Nodular extension of the mass along the expected course of the nerve with stretching of the nerve may be seen and indicates the neural origin of the mass.

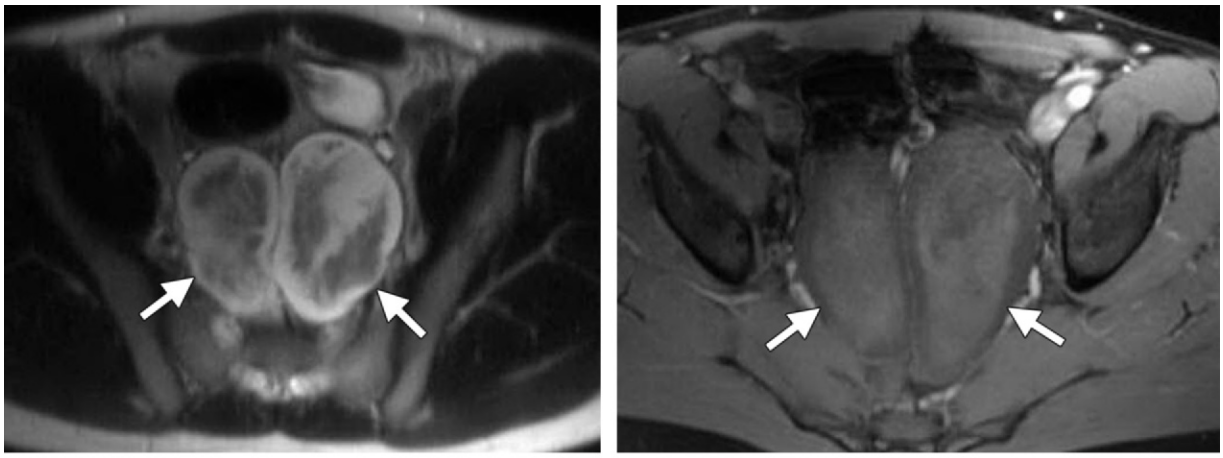

a. b.

Figure 21. Plexiform neurofibromas in a patient with neurofibromatosis type 1. **(a)** Axial T2-weighted MR image shows two well-defined lesions with a targetlike pattern (peripheral high signal intensity and central low signal intensity) (arrows) in the pelvis. Note the linear pattern of hypointensity within the lesions, a finding that is characteristic of plexiform neurofibroma. **(b)** On an axial gadolinium-enhanced T1-weighted MR image, the lesions (arrows) show moderate enhancement centrally and minimal or no enhancement peripherally.

Plexiform Neurofibroma

Neurofibromas are unencapsulated neurogenic tumors that arise from the nerve sheath. They account for about 5% of all benign soft-tissue neoplasms. Plexiform neurofibroma is a specific subtype of neurofibroma that is seen almost exclusively in neurofibromatosis type 1, and rarely as an isolated finding (17). Most neurofibromas manifest in the 2nd to 4th decades of life, whereas patients with neurofibromatosis type 1 present at an earlier age. Retroperitoneal plexiform neurofibromas are usually bilateral and symmetric, which helps differentiate these benign neoplasms from malignant nerve sheath tumors (71).

Neurofibromas manifest as well-defined, homogeneously hypoechoic masses at US. Plexiform neurofibromas are hypoattenuating relative to soft tissue at CT due to the presence of lipid-rich Schwann cells, adipocytes, and myxoid change (71). Pelvic plexiform neurofibromas tend to be large and may appear as hypoattenuating, hypovascular infiltrative masses or as intensely enhancing soft-tissue masses (72). The typical imaging appearance at T2-weighted MR imaging includes a targetlike pattern consisting of peripheral high signal intensity (representing the myxoid stroma) and central low signal intensity (representing fibrous-collagenous tissue) (Fig 21) (66). A targetlike pattern may also be seen at CT and is seen in up to 52% of benign neurogenic tumors (neurofibroma or schwannoma). In contrast, malignant peripheral nerve sheath tumors do not show a targetlike pattern at imaging. Marked T2 hyperintensity with multiple linear hypointense areas has been described as a specific finding of pelvic plexiform neurofibroma that may help differentiate it from other neoplasms (73).

Teaching Point

Leiomyomas in the Pelvic Retroperitoneum

Retroperitoneal leiomyomatosis-leiomyoma is an unusual growth pattern of leiomyoma. Retroperitoneal leiomyoma may originate from remnants of müllerian or wolffian ducts in the retroperitoneal space, from hormonally sensitive smooth muscle elements in the retroperitoneum, or as a result of metastasis from uterine leiomyoma (74). Up to 40% of patients with retroperitoneal leiomyoma have either a concurrent or a remote history of uterine leiomyoma. Parasitic leiomyoma is a distinct entity that arises when a leiomyoma becomes adherent to the retroperitoneal connective tissue, develops an auxillary blood supply, and loses its attachment with the uterus (75). Occasionally, a cervical leiomyoma may grow into the retroperitoneal space, simulating a primary pelvic retroperitoneal mass at imaging.

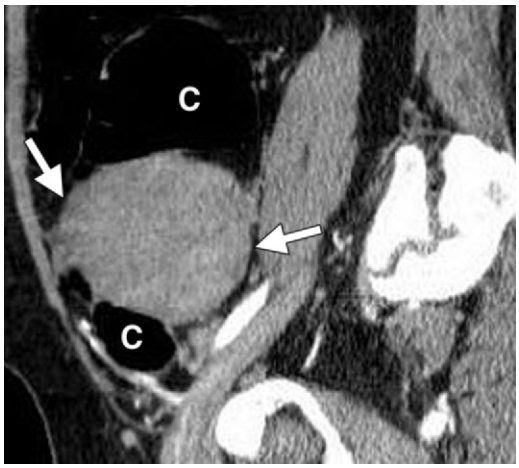

Figure 22. Leiomyoma. Sagittal contrast-enhanced CT scan shows a homogeneously enhancing mass in the right lower quadrant (arrows) that displaces the cecum *(C)* anteriorly, thereby confirming the retroperitoneal location of the mass. Surgical excision helped confirm the diagnosis of retroperitoneal leiomyoma.

Figure 23. Parasitic leiomyoma. Sagittal T2-weighted MR image shows an oval hypointense lesion (arrows) in the pelvic retroperitoneal space. The lesion proved to be a parasitic leiomyoma at surgical excision.

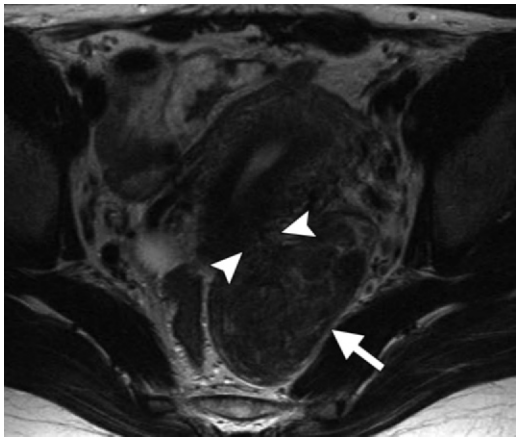

Figure 24. Retroperitoneal extension of cervical leiomyoma. Axial T2-weighted MR image shows a large, hypointense pelvic retroperitoneal mass (arrow). Arrowheads indicate a stalk connecting the mass with the cervix. A preoperative diagnosis of retroperitoneal extension or growth of cervical leiomyoma was made. Surgical excision helped confirm the diagnosis.

At CT, retroperitoneal leiomyoma appears as a well-defined homogeneous mass in the pelvic retroperitoneum (Fig 22). Calcification is rare. At MR imaging, retroperitoneal leiomyoma demonstrates low T2 signal intensity, intermediate T1 signal intensity, and variable enhancement following contrast material administration (Fig 23) (74). Primary retroperitoneal leiomyomas can be differentiated from retroperitoneal growth of cervical leiomyoma in that the latter usually shows contiguity with the cervix (Fig 24).

Conclusions

A broad spectrum of solid, cystic, vascular, myxoid, calcified, and fatty lesions occur as primary masses in the pelvic retroperitoneum. Accurate detection and characterization of pelvic masses on the basis of anatomic distribution as well as demographic and imaging features (Table) allows optimal patient management. Cross-sectional imaging modalities help differentiate the more common gynecologic neoplasms from the rarer masses discussed in this article. The tissue-specific multiplanar capability of high-resolution MR imaging permits better tumor localization and internal characterization, thereby serving as a road map for surgery.

Key Features of Uncommon Primary Pelvic Retroperitoneal Masses

Type of Mass	Demographic Features	Imaging Features
Cystic		
Serous epithelial neoplasms	Commonly seen in middle-aged women with nonspecific symptoms	Cystic pelvic retroperitoneal mass; mural nodules and solid components favor malignancy
Ancient schwannoma	Commonly seen in elderly patients, is often indolent and asymptomatic	Well-defined complex cystic mass with variable enhancement
Lymphangioma	Occurs in isolation or as a part of Klippel-Trénaunay-Weber syndrome, asymptomatic or nonspecific pressure symptoms	Uni- or multilocular cystic mass, crosses from one anatomic compartment to another
Tailgut cyst	More common in middle-aged women, may manifest at any age, infection and malignant degeneration are recognized complications	Uni- or multilocular cystic mass, typically multicystic, asymmetric irregular wall thickening and heterogeneous enhancement favor malignancy
Vascular or hypervascular		
SFT	Commonly seen in the 5th decade of life, no gender predilection, typically asymptomatic, 5% of patients present with hypoglycemia	Hypervascular mass with a fibrous component, intense arterial enhancement that persists on delayed phase images
Extraadrenal pheochromocytoma or paraganglioma	Symptoms of excess catecholamine, elevated levels of urine vanillylmandelic acid and serum norepinephrine	Located below the aortic bifurcation; T2 hyperintense; hypervascular mass with increased uptake at ^{123}I or ^{131}I MIBG, ^{111}In pentetreotide, and FDOPA PET
Congenital pelvic AVM	Indolent with a long latency period; pelvic pain, vaginal bleeding, hematuria, and a pulsatile mass seen at presentation	Multiple feeding vessels commonly arise from the internal iliac artery with early opacification of the draining vein, angiography is the standard of reference, MR imaging is the noninvasive imaging modality of choice
Klippel-Trénaunay-Weber syndrome	Sporadic, present at birth, equal gender distribution	Multiple pelvic venous varicosities in contiguity with genitalia or limbs, multiple pelvic phleboliths seen at CT, coexistent lymphatic malformation
Extraintestinal GIST	Extremely rare, can occur over a wide age range (31–82 y), female predilection	Hypervascular mass with hypointense areas representing a fibrous component may be seen on T2-weighted images

(continues)

References

1. Auh YH, Rubenstein WA, Schneider M, Reckler JM, Whalen JP, Kazam E. Extraperitoneal paravesical spaces: CT delineation with US correlation. Radiology 1986;159(2):319–328.
2. O'Connell AM, Duddy L, Lee C, Lee MJ. CT of pelvic extraperitoneal spaces: an anatomical study in cadavers. Clin Radiol 2007;62(5):432–438.
3. Zhang C, Ding ZH, Li GX, Yu J, Wang YN, Hu YF. Perirectal fascia and spaces: annular distribution pattern around the mesorectum. Dis Colon Rectum 2010;53(9):1315–1322.
4. Smart OC, Gedroyc WG, Regan LR. Pelvic schwannoma: a retroperitoneal tumour mimicking uterine leiomyoma. J Obstet Gynaecol 2007;27(1):94–96.
5. Foshager MC, Hood LL, Walsh JW. Masses simulating gynecologic diseases at CT and MR imaging. RadioGraphics 1996;16(5):1085–1099.

Key Features of Uncommon Primary Pelvic Retroperitoneal Masses (continued)

Type of Mass	Demographic Features	Imaging Features
Fat-containing		
Lipoma or liposarcoma	Can be asymptomatic for a long period of time, typically occurs in elderly patients	Purely fat-containing mass suggests lipoma; solid components, local invasion, or distant metastasis favors liposarcoma
Myelolipoma	Asymptomatic, typically occurs in elderly women	Presacral mass containing fat and soft tissue
Presacral teratoma	Common in children but very rare in adults, women more commonly affected than men, asymptomatic or associated with recurrent pilonidal infections	Contains fat, cystic component, and calcification; can undergo malignant degeneration; surgical excision necessary to exclude malignancy
Calcified		
Iatrogenic (lymphocele or rejected transplant kidney)	Prior surgery (transplantation, lymphadenectomy)	Lymphoceles are cystic lesions with a thin wall, long-standing lesions rarely undergo calcification; atrophic rejected transplant kidney can undergo cortical nephrocalcinosis, evidence of vascular anastomosis with iliac vessels is a clue to the diagnosis
Uncommon primary pelvic retroperitoneal sarcoma	Nonspecific clinical presentation, more common in middle-aged and elderly patients	Large heterogeneous masses with calcification, may show local invasion or distant metastases
Myxoid		
Myxoma	Typically seen in the 5th decade of life, female predilection	Very high T2 signal intensity, mild or no enhancement, noncystic appearance at US, may show multiple internal septa
Schwannoma	Asymptomatic, may be unusually large at presentation	High T2 signal intensity with moderate enhancement, located along expected course of nerve
Plexiform neurofibroma	Typically associated with NF-1	Targetlike pattern at MR imaging, bilateral symmetric pelvic masses, may show widening of neural foramina

Note.—FDOPA = fluorodihydroxyphenylalanine, NF-1 = neurofibromatosis type 1, PET = positron emission tomography, US = ultrasonography.

6. Kayikcioglu F, Haberal A, Caglar G, Koc S, Gunes M. Analysis of retroperitoneal tumors operated on in a gynecology clinic. J Obstet Gynaecol Res 2005; 31(4):323–328.
7. Demir MK, Unlu E, Genchellac H, Temizoz O, Ozdemir H. Primary serous papillary carcinoma of the retroperitoneum: magnetic resonance imaging findings with pathologic correlation. Australas Radiol 2007;51(spec no):B71–B73.
8. Ulbright TM, Morley DJ, Roth LM, Berkow RL. Papillary serous carcinoma of the retroperitoneum. Am J Clin Pathol 1983;79(5):633–637.
9. Kurosaki Y, Kuramoto K. Serous cystadenocarcinoma of the retroperitoneum: CT and sonographic appearance. Clin Radiol 1998;53(12):916–918.
10. Caruncho M, Pombo F, Arnal-Monreal F. Primary retroperitoneal serous cystadenocarcinoma of 'ovarian-type': US and CT findings. Eur J Radiol 1993; 17(2):115–116.
11. Fujiwara K, Oda T, Suzuki S, Kohno I, Hirokawa M. Primary serous adenocarcinoma of the retroperitoneum with a response to platinum-based chemotherapy: a case report. Int J Gynecol Cancer 1999;9 (2):170–172.
12. Kaku M, Ohara N, Seima Y, et al. A primary retroperitoneal serous cystadenocarcinoma with clinically aggressive behavior. Arch Gynecol Obstet 2004;270 (4):302–306.

13. Dahl I. Ancient neurilemmoma (schwannoma). Acta Pathol Microbiol Scand [A] 1977;85(6):812–818.
14. Hide IG, Baudouin CJ, Murray SA, Malcolm AJ. Giant ancient schwannoma of the pelvis. Skeletal Radiol 2000;29(9):538–542.
15. Loke TK, Yuen NW, Lo KK, Lo J, Chan JC. Retroperitoneal ancient schwannoma: review of clinicoradiological features. Australas Radiol 1998;42(2):136–138.
16. McCluggage WG, Bharucha H. Primary pulmonary tumours of nerve sheath origin. Histopathology 1995;26(3):247–254.
17. Isobe K, Shimizu T, Akahane T, Kato H. Imaging of ancient schwannoma. AJR Am J Roentgenol 2004;183(2):331–336.
18. Kobayashi H, Kotoura Y, Sakahara H, et al. Schwannoma of the extremities: comparison of MRI and pentavalent technetium-99m-dimercaptosuccinic acid and gallium-67-citrate scintigraphy. J Nucl Med 1994;35(7):1174–1178.
19. Rasbridge SA, Browse NL, Tighe JR, Fletcher CD. Malignant nerve sheath tumour arising in a benign ancient schwannoma. Histopathology 1989;14(5):525–528.
20. Davidson AJ, Hartman DS. Lymphangioma of the retroperitoneum: CT and sonographic characteristics. Radiology 1990;175(2):507–510.
21. Erdem S, Iskender C, Avsar AF, Altundag OB, Ustunyurt E. Benign cystic lymphangioma presenting as a pelvic mass. J Obstet Gynaecol Res 2006;32(6):628–630.
22. Iyer R, Eftekhari F, Varma D, Jaffe N. Cystic retroperitoneal lymphangioma: CT, ultrasound and MR findings. Pediatr Radiol 1993;23(4):305–306.
23. Allen JG, Riall TS, Cameron JL, Askin FB, Hruban RH, Campbell KA. Abdominal lymphangiomas in adults. J Gastrointest Surg 2006;10(5):746–751.
24. Guinier D, Denue PO, Mantion GA. Intra-abdominal cystic lymphangioma. Am J Surg 2006;191(5):706–707.
25. Johnson AR, Ros PR, Hjermstad BM. Tailgut cyst: diagnosis with CT and sonography. AJR Am J Roentgenol 1986;147(6):1309–1311.
26. Yang DM, Park CH, Jin W, et al. Tailgut cyst: MRI evaluation. AJR Am J Roentgenol 2005;184(5):1519–1523.
27. Liessi G, Cesari S, Pavanello M, Butini R. Tailgut cysts: CT and MR findings. Abdom Imaging 1995;20(3):256–258.
28. Lim KE, Hsu WC, Wang CR. Tailgut cyst with malignancy: MR imaging findings. AJR Am J Roentgenol 1998;170(6):1488–1490.
29. Prasad AR, Amin MB, Randolph TL, Lee CS, Ma CK. Retrorectal cystic hamartoma: report of 5 cases with malignancy arising in 2. Arch Pathol Lab Med 2000;124(5):725–729.
30. Peixoto Callejo I. Peritoneal solitary fibrous tumour (SFT): long-term survival of recurrent and metastasized SFT treated with cytoreductive surgery and intraperitoneal chemotherapy. Clin Transl Oncol 2009;11(4):250–252.
31. Wagner S, Greco F, Hamza A, Hoda RM, Holzhausen HJ, Fornara P. Retroperitoneal malignant solitary fibrous tumor of the small pelvis causing recurrent hypoglycemia by secretion of insulin-like growth factor 2. Eur Urol 2009;55(3):739–742.
32. Shanbhogue AK, Prasad SR, Takahashi N, Vikram R, Zaheer A, Sandrasegaran K. Somatic and visceral solitary fibrous tumors in the abdomen and pelvis: cross-sectional imaging spectrum. RadioGraphics 2011;31(2):393–408.
33. Insabato L, Siano M, Somma A, Gentile R, Santangelo M, Pettinato G. Extrapleural solitary fibrous tumor: a clinicopathologic study of 19 cases. Int J Surg Pathol 2009;17(3):250–254.
34. Kawamura S, Nakamura T, Oya T, et al. Advanced malignant solitary fibrous tumor in pelvis responding to radiation therapy. Pathol Int 2007;57(4):213–218.
35. Daigeler A, Lehnhardt M, Langer S, et al. Clinicopathological findings in a case series of extrathoracic solitary fibrous tumors of soft tissues. BMC Surg 2006;6:10.
36. Subramanian A, Maker VK. Organs of Zuckerkandl: their surgical significance and a review of a century of literature. Am J Surg 2006;192(2):224–234.
37. Salanitri J, Smith P, Schlicht S. Multifocal malignant extra-adrenal paragangliomas of the organ of Zuckerkandl and urinary bladder. Australas Radiol 2001;45(2):229–232.
38. Qiao HS, Feng XL, Yong L, Yong Z, Lian ZJ, Ling LB. The MRI of extraadrenal pheochromocytoma in the abdominal cavity. Eur J Radiol 2007;62(3):335–341.
39. Hoefnagel CA. Metaiodobenzylguanidine and somatostatin in oncology: role in the management of neural crest tumours. Eur J Nucl Med 1994;21(6):561–581.
40. Rao AB, Koeller KK, Adair CF. Paragangliomas of the head and neck: radiologic-pathologic correlation. RadioGraphics 1999;19(6):1605–1632.
41. Fottner C, Helisch A, Anlauf M, et al. 6-18F-fluoro-L-dihydroxyphenylalanine positron emission tomography is superior to 123I-metaiodobenzyl-guanidine scintigraphy in the detection of extraadrenal and hereditary pheochromocytomas and paragangliomas: correlation with vesicular monoamine transporter expression. J Clin Endocrinol Metab 2010;95(6):2800–2810.
42. Lenders JW, Pacak K, Walther MM, et al. Biochemical diagnosis of pheochromocytoma: which test is best? JAMA 2002;287(11):1427–1434.
43. Gomes MM, Bernatz PE. Arteriovenous fistulas: a review and ten-year experience at the Mayo Clinic. Mayo Clin Proc 1970;45(2):81–102.

44. Calligaro KD, Sedlacek TV, Savarese RP, Carneval P, DeLaurentis DA. Congenital pelvic arteriovenous malformations: long-term follow-up in two cases and a review of the literature. J Vasc Surg 1992;16 (1):100–108.
45. Smith MR. Pulsatile pelvic masses: options for evaluation and management of pelvic arteriovenous malformations. Am J Obstet Gynecol 1995;172(6): 1857–1862; discussion 1862–1863.
46. Wei CJ, Tseng HS, Wu MH, Tiu CM, Yang MJ, Chang CY. Congenital pelvic arteriovenous malformation: two cases and MR findings. Eur J Obstet Gynecol Reprod Biol 2003;108(2):226–228.
47. Game X, Berlizot P, Hassan T, et al. Congenital pelvic arteriovenous malformation in male patients: a rare cause of urological symptoms and role of embolization. Eur Urol 2002;42(4):407–412.
48. Jacob AG, Driscoll DJ, Shaughnessy WJ, Stanson AW, Clay RP, Gloviczki P. Klippel-Trénaunay syndrome: spectrum and management. Mayo Clin Proc 1998;73(1):28–36.
49. Berry SA, Peterson C, Mize W, et al. Klippel-Trenaunay syndrome. Am J Med Genet 1998;79(4): 319–326.
50. James CA, Allison JW, Waner M. Klippel-Trénaunay syndrome. RadioGraphics 1999;19(4):1093–1096.
51. Reith JD, Goldblum JR, Lyles RH, Weiss SW. Extragastrointestinal (soft tissue) stromal tumors: an analysis of 48 cases with emphasis on histologic predictors of outcome. Mod Pathol 2000;13(5):577–585.
52. Hsiao JC, Yang YC, Lin WC, Lin YN, Wang KG. Primary retroperitoneal liposarcoma mimicking ovarian cancer: a case report. Zhonghua Yi Xue Za Zhi (Taipei) 1998;61(5):295–300.
53. Kuppuvelumani P, Rachagan SP, Syed N, Kumar G, Cheah PL. Rare case of huge retroperitoneal liposarcoma presenting as a gynaecological problem. Eur J Obstet Gynecol Reprod Biol 1993;48(3): 220–222.
54. Susini T, Taddei G, Massi D, Massi G. Giant pelvic retroperitoneal liposarcoma. Obstet Gynecol 2000; 95(6 pt 2):1002–1004.
55. Szklaruk J, Tamm EP, Choi H, Varavithya V. MR imaging of common and uncommon large pelvic masses. RadioGraphics 2003;23(2):403–424.
56. Kammen BF, Elder DE, Fraker DL, Siegelman ES. Extraadrenal myelolipoma: MR imaging findings. AJR Am J Roentgenol 1998;171(3):721–723.
57. Singla AK, Kechejian G, Lopez MJ. Giant presacral myelolipoma. Am Surg 2003;69(4):334–338.
58. Bryant P, Leditschke JF, Hewett P. Hereditary presacral teratoma. Aust N Z J Surg 1996;66(6): 418–420.
59. Bull J Jr, Yeh KA, McDonnell D, Caudell P, Davis J. Mature presacral teratoma in an adult male: a case report. Am Surg 1999;65(6):586–591.
60. Kim JK, Jeong YY, Kim YH, Kim YC, Kang HK, Choi HS. Postoperative pelvic lymphocele: treatment with simple percutaneous catheter drainage. Radiology 1999;212(2):390–394.
61. Secil M, Mungan U, Yorukoglu K, Dicle O. Retroperitoneal extraskeletal osteosarcoma. Radiology 2005;237(3):880–883.
62. Ireland DC, Soule EH, Ivins JC. Myxoma of somatic soft tissues: a report of 58 patients, 3 with multiple tumors and fibrous dysplasia of bone. Mayo Clin Proc 1973;48(6):401–410.
63. Stout AP. Myxoma, the tumor of primitive mesenchyme. Ann Surg 1948;127(4):706–719.
64. Allen PW. Myxoma is not a single entity: a review of the concept of myxoma. Ann Diagn Pathol 2000; 4(2):99–123.
65. Murphey MD, McRae GA, Fanburg-Smith JC, Temple HT, Levine AM, Aboulafia AJ. Imaging of soft-tissue myxoma with emphasis on CT and MR and comparison of radiologic and pathologic findings. Radiology 2002;225(1):215–224.
66. Murphey MD, Smith WS, Smith SE, Kransdorf MJ, Temple HT. Imaging of musculoskeletal neurogenic tumors: radiologic-pathologic correlation. RadioGraphics 1999;19(5):1253–1280.
67. Lane RH, Stephens DH, Reiman HM. Primary retroperitoneal neoplasms: CT findings in 90 cases with clinical and pathologic correlation. AJR Am J Roentgenol 1989;152(1):83–89.
68. Kim SH, Choi BI, Han MC, Kim YI. Retroperitoneal neurilemoma: CT and MR findings. AJR Am J Roentgenol 1992;159(5):1023–1026.
69. Kinoshita T, Naganuma H, Ishii K, Itoh H. CT features of retroperitoneal neurilemmoma. Eur J Radiol 1998;27(1):67–71.
70. Rha SE, Byun JY, Jung SE, Chun HJ, Lee HG, Lee JM. Neurogenic tumors in the abdomen: tumor types and imaging characteristics. RadioGraphics 2003;23(1):29–43.
71. Bass JC, Korobkin M, Francis IR, Ellis JH, Cohan RH. Retroperitoneal plexiform neurofibromas: CT findings. AJR Am J Roentgenol 1994;163(3): 617–620.
72. Fortman BJ, Kuszyk BS, Urban BA, Fishman EK. Neurofibromatosis type 1: a diagnostic mimicker at CT. RadioGraphics 2001;21(3):601–612.
73. Ros PR, Eshaghi N. Plexiform neurofibroma of the pelvis: CT and MRI findings. Magn Reson Imaging 1991;9(3):463–465.
74. Fasih N, Prasad Shanbhogue AK, Macdonald DB, et al. Leiomyomas beyond the uterus: unusual locations, rare manifestations. RadioGraphics 2008;28 (7):1931–1948.
75. Rader JS, Binette SP, Brandt TD, Sreekanth S, Chhablani A. Ileal hemorrhage caused by a parasitic uterine leiomyoma. Obstet Gynecol 1990;76(3 pt 2):531–534.

RadioGraphics

Uncommon Primary Pelvic Retroperitoneal Masses in Adults: A Pattern-based Imaging Approach

Alampady K. Shanbhogue, MD • Najla Fasih, FRCR • David B. Macdonald, MD • Adnan M. Sheikh, MD • Christine O. Menias, MD • Srinivasa R. Prasad, MD

RadioGraphics 2012; 32:795–817 • **Published online** 10.1148/rg.323115020 • **Content Codes:** CT GI MR

Page 801
The presence of asymmetric irregular wall thickening with heterogeneous enhancement following contrast material administration raises suspicion for malignant change within a duplication cyst.

Page 801
At imaging, SFTs appear as well-defined masses with intense heterogeneous enhancement that persists on delayed phase images obtained following contrast material administration. Areas of central low attenuation representing necrosis, hemorrhage, or cystic change may be seen.

Page 803
MR imaging is the noninvasive imaging modality of choice for the diagnosis of pelvic AVMs and the delineation of their size and extent (46). The anatomic details seen at MR imaging (including the relationship of AVMs to adjacent pelvic structures) help in preoperative evaluation and preembolization planning.

Page 806
The differentiation of presacral myelolipoma from other fat-containing lesions may not always be possible with imaging alone. The fact that presacral myelolipoma occurs predominantly in elderly women is the single most distinguishing feature that helps differentiate this tumor from other fat-containing presacral lesions.

Page 812 (Figure on page 812)
The typical imaging appearance at T2-weighted MR imaging includes a targetlike pattern consisting of peripheral high signal intensity (representing the myxoid stroma) and central low signal intensity (representing fibrous-collagenous tissue) (Fig 21) (66).